Supporting Information for

A Natural Topological Insulator

P. Gehring[1], H. M. Benia[1], Y. Weng[2], R. Dinnebier[1], C. R. Ast[1], M. Burghard[1] and K. Kern[1,3]*

[1]Max-Planck-Institut für Festkörperforschung, Heisenbergstrasse 1, D-70569 Stuttgart (Germany)

[2]Institut für Materialwissenschaft, Universität Stuttgart, Heisenbergstrasse 3, D-70569 Stuttgart (Germany)

[3]Institut de Physique de la Matière Condensée, Ecole Polytechnique Fédérale de Lausanne, CH-1015 Lausanne (Switzerland)

Semi-quantitative ICP analysis

We performed a semi-quantitative analysis of the mineral to detect possible impurities. The results are shown in **Table S1**.

Table S1. Results of the semi-quantitative analysis

Element	***wt.%***	***Element***	***wt.%***	***Element***	***wt.%***
Al	1.28	Cr	0.02	Ni	0.05
As	0.73	Cu	0.02	Ti	0.02
Au	0.11	Fe	0.23	Zn	0.01
Ba	0.01	Mg	0.58	Zr	0.04
Co	0.12	Na	0.18		

XRD

Indexing[1] of the recorded spectra led to two similar R-centered trigonal unit cells for with lattice parameters given in **Table S2**, suggesting the parallel occurrence of two Kawazulite phases with different distribution of elements. The major phase (I) has a slightly smaller unit cell as the minor phase (II). Starting coordinates for both crystal structures of Kawazulite were taken from the literature[2]. Rietveld refinement[3] was performed using the program TOPAS Version 4.2 (Bruker AXS, 2010). The peak profiles and precise lattice parameters were determined by a LeBail fit[4] using the fundamental parameter approach of TOPAS[5]. From elemental analysis, a fully occupied bismuth position could be anticipated, allowing the other occupancies to be correctly refined. A full quantitative Rietveld analysis of the Kawazulite sample revealed a fraction of 89.6(4) wt% for (I) and 10.4(4) of (II). Despite the use of Debye-Scherrer geometry, a small amount of preferred orientation was detected which refined to identical values for both phases using the March-Dollase formalism[6]. Agreement factors (R-values) are listed in **Table S2** and the refined coordinates are given in **Table S3**.

Table S2. Crystallographic data for the two Kawazulite phases

	$Bi_2(Se_{0.2}S_{0.74})(Te_{0.61}Se_{0.39})_2$	$Bi_2(Se_{0.59}Te_{0.41})Te_2$
Space group	$R\bar{3}m$	$R\bar{3}m$
Cell parameters [Å,°]	a = 4.2537(2)	a = 4.3648(8)
	c = 29.704(2)	c = 30.424(8)
Cell volume [$Å^3$]	V = 465.45(6)	V = 502.0(2)
Z	3	3
T [K]	300	300
Formula weight [g/mol]	2038	2340
ρ_{calc} ($\rho_{measured}$) [g/cm^3]	7.27(1)	7.74(15)
Radiation source/□ [Å]	0.55941	0.55941
R_{exp} [%][a]	2.47	2.47
R_{wp}[%] [a]	5.00	5.00
R_p [%][a]	3.83	3.83
R_{Bragg} [%][a]	3.02	2.00
GoF	2.03	2.03

[a] as defined in TOPAS.

Table S3a. Atomic positions and isotropic thermal parameters of Kawazulite phase (I)

Atom	Wyck.	x	y	z	rel. occ.	U(eq) [$Å^2$]
Bi	6*f*	0	0	0.41125(4)	1	0.70(4)
S/Se	3*c*	0	0	0	0.70(4)/0.30(4)	0.70(4)
Te/Se	6*f*	0	0	0.19787(9)	0.61(1)/0.39(1)	0.70(4)

Table S3b. Atomic positions and isotropic thermal parameters of Kawazulite phase (II)

Atom	Wyck.	x	y	z	rel. occ.	U(eq) [Å^2]
Bi	6*f*	0	0	0.4083(4)	1	0.70(4)
Te/Se	3*c*	0	0	0	0.4(2)/0.6(2)	0.70(4)
Te	6*f*	0	0	0.1994(8)	1	0.70(4)

XPS

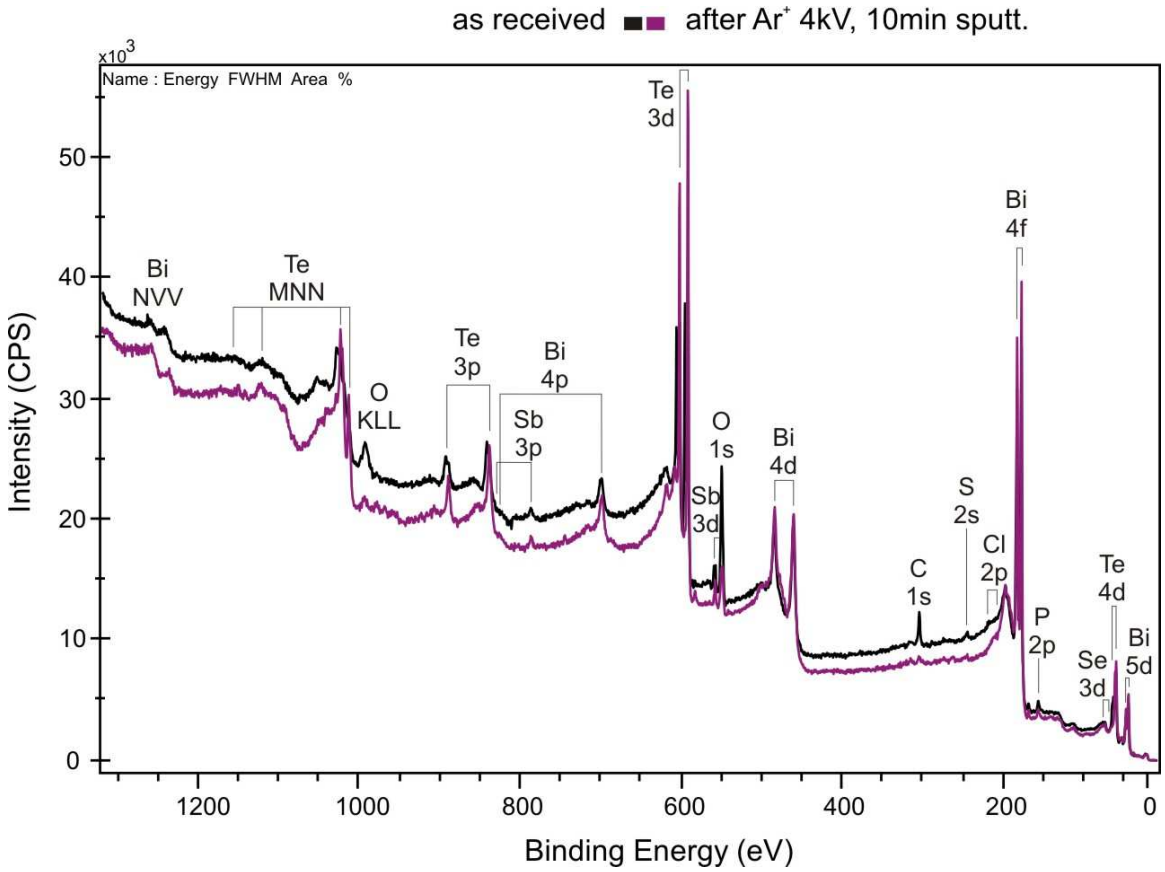

Figure S1. Results of the XPS measurements as received (black curve) and after 10min of Ar sputtering (purple curve). The main elements Bi, Te, Se, S and Sb can be detected.

Additional electrical transport data

Table S4. Sheet thickness, sheet resistance, carrier density and mobility values for several devices

Sample-#	*d (nm)*	R_s *(Ω)*	*n* (m^{-2})	μ (cm^2/Vs)
1	7	-	$1.72 \cdot 10^{17}$	-
2	70	1277	$1.88 \cdot 10^{17}$	260
3	17	2437	$1.24 \cdot 10^{17}$	393
4	17	2013	$1.81 \cdot 10^{17}$	270
5	12	2047	$3.80 \cdot 10^{16}$	1272
6	46	3641	$5.20 \cdot 10^{16}$	934

WAL data

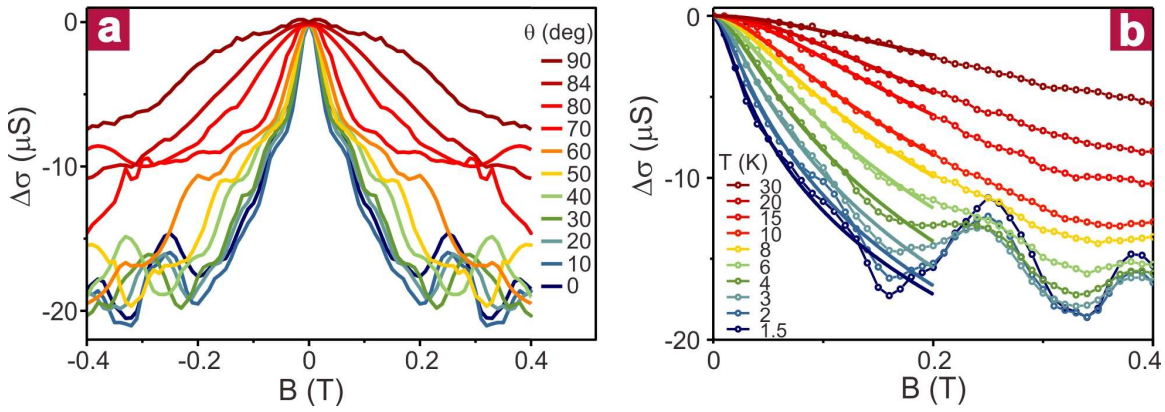

Figure S2. (a) Low field magnetoconductance of the sample discussed in the main text at different tilting angles θ. (b) Low field magnetoconductance data at different temperatures. The solid lines in the range $0 < B < 0.2$ T represent data fits obtained by the HLN equation.

UCF data

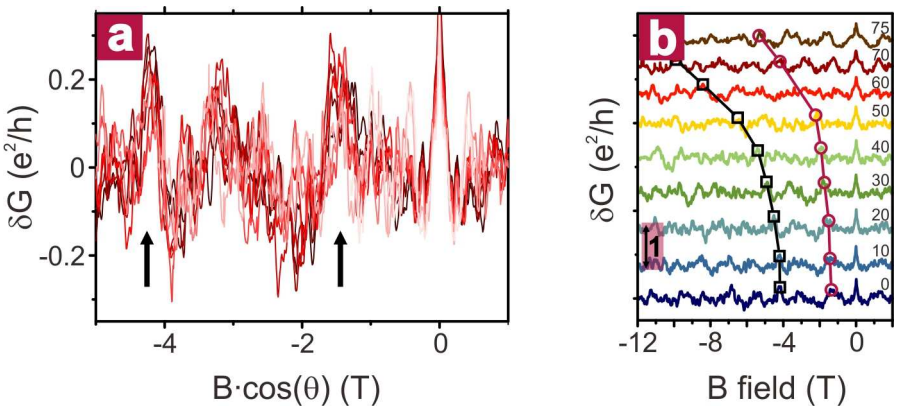

Figure S3. (a) UCF as a function of the *B*-field component normal to the sample surface. (b) UCF at different angles. The squares/circles mark the *B*-field position of the tow characteristic features (marked with arrows in a) of the UCF at different angles. These positions are also shown in Figure 4 (e) of the main text.

REFERENCES

1. Coelho, A. A. *J Appl Crystallogr* **2003,** 36, 86-95.

2. Nakajima, S. *Journal of Physics and Chemistry of Solids* **1963,** 24, (3), 479-485.

3. Rietveld, H. M. *J Appl Crystallogr* **1969,** 2, 65.

4. Lebail, A.; Duroy, H.; Fourquet, J. L. *Mater Res Bull* **1988,** 23, (3), 447-452.

5. R.W. Cheary, A. A. C., J.P. Cline. *J. Res. Natl. Inst. Stand. Technol.* **2005,** 109, 1.

6. March, A. *Z Kristallogr* **1932,** 81, (3/4), 285-297.